Title: Partitioning of root respiration into growth, maintenance, and ion uptake components in a young larch-dominated forest

Authors: Takashi Hirano[a, *], Rui Cui[b], Lifei Sun[a, c], Munemasa Teramoto[c, d] and Naishen Liang[c]

[a] Research Faculty of Agriculture, Hokkaido University, Sapporo 060-8589, Japan

[b] Graduate School of Agriculture, Hokkaido University, Sapporo 060-8584, Japan

[c] Center for Global Environmental Research, National Institute for Environmental Studies, Tsukuba 305-8506, Japan

[d] Arid Land Research Center, Tottori University, Tottori 680-0001, Japan

*Correspondence: hirano@env.agr.hokudai.ac.jp, tel/fax +84-11 706 3689

Abstract

Purpose: Fine roots play an essential role in global carbon cycles, but phenological variations in root function and metabolism are poorly understood. To illustrate the dynamics of fine root function and metabolism in the field, we partitioned root respiration (R_r) into growth (R_g), maintenance (R_m), and ion uptake (R_{ion}) components using a modified traditional model.

Methods: A year-round experiment was conducted in a young larch-dominated forest regrowing on bare soil. Soil respiration was measured with a chamber method and partitioned into R_r and heterotrophic respiration by trenching. Fine root biomass and production were measured simultaneously. Using the field data, the model was parameterized, and R_r was further partitioned.

Results: Annually, R_r (210–253 g C m^{-2} yr^{-1}) accounts for 45–47% of the total soil respiration. The contribution of fine root R_g, fine root R_m, coarse root R_m, and fine root R_{ion} were 26–40, 46–51, 10–16, and 12%, respectively. The R_g contribution showed a clear seasonal variation, with a peak in mid-spring and a minimum in early fall, mainly because of different seasonality between fine root production and soil temperature.

Conclusion: The model parameters were consistent with those from our previous study conducted by the same method in the same site. Thus, we believe that our approach was robust under a relatively simple condition. However, our growth respiration parameter resulting from only field data was much higher than those from laboratory experiments. To further improve our understanding of root respiration, more field data should be accumulated.

Keywords: Chamber, fine root, root biomass, root production, sap flow, soil respiration

1. Introduction

Soil respiration (R_s) is composed of autotrophic respiration by plant roots (R_r) and heterotrophic respiration (R_h) by soil microorganisms and fauna. R_r corresponds to mycorrhizosphere respiration consisting of living root, rhizomicrobial, and mycorrhizal respiration. R_h is equivalent to the decomposition of soil organic matter (SOM) and root litter by soil microbes (Kuzyakov 2006; Moyano et al. 2009). The global annual R_r was reported to be approximately 44 Pg C yr^{-1} (Tang et al. 2019), which is approximately fourfold greater than anthropogenic carbon emissions (Friedlingstein et al. 2020). The contribution of R_r to R_s varies from 10 to 90% in forest ecosystems (Hanson et al. 2000) but is typically 45–50% annually (Subke et al. 2006). Because R_r and R_h respond differently to environmental factors, such as temperature and water content (Boone et al. 1998; Lavigne et al. 2004; Scott-Denton et al. 2006), R_s should be partitioned into two components to understand ecosystem-scale carbon cycling.

Plant root systems are composed of fine and coarse roots that serve contrasting functions. Fine roots, commonly defined as roots thinner than 2 mm in diameter (Brunner et al. 2013; Finér et al. 2011b), absorb water and nutrients from the soil. Despite their small biomass, fine roots have a large net primary production (NPP), accounting for 22% of terrestrial NPP (McCormack et al. 2015a) because of their fast turnover rates (Brunner et al. 2013; Finér et al. 2011b). Thus, fine roots play a dominant role in belowground carbon cycling (Finér et al. 2011b; Richter et al. 1999). Although fine root phenology strongly influences belowground carbon dynamics, seasonality and variability in fine root function are poorly understood (Abramoff and Finzi 2015; McCormack et al. 2014; Radville et al. 2016).

Autotrophic respiration is further separated into growth (R_g) and maintenance (R_m) components (Amthor 2000; McCree 1974; Penning de Vries 1974; Thornley 1970) and sometimes into an ion uptake component (R_{ion}) for fine root respiration (Chapin et al. 2011; Johnson 1990; Lambers et al. 2008) using a conceptual model. In the model, R_g, R_m, and R_{ion} were linearly correlated with growth (production), biomass, and ion uptake, respectively. However, the model has been criticized for its weak scientific basis in quantitative partitioning into R_g and R_m (Cannell and Thornley 2000; Sweetlove et al. 2013; Thornley 2011), although experimental results indicate that the model is useful for understanding ecological control of autotrophic respiration (Chapin et al. 2011; Lambers et al. 2008). Most terrestrial biosphere models do not explicitly incorporate root respiration because of a lack of mechanistic

respiration models (Collalti et al. 2020; Hopkins et al. 2013; Sweetlove et al. 2013; Warren et al. 2015). Respiration is frequently estimated from other processes using correlation (Sweetlove et al. 2013), and important processes contributing to respiration have been oversimplified (Ballantyne et al. 2017). The partitioning model is effective for understanding and quantifying intrinsic processes, such as acclimation to warming.

The partitioning model has been applied to R_r measured through laboratory experiments in controlled environments (Lambers et al. 2008; Thongo M'Bou et al. 2010). In the field, (George et al. 2003) partitioned R_r into R_g, R_m, and R_{ion} (nitrogen uptake), based on laboratory data and a short-term field experiment. (Sun et al. 2020) conducted a year-round experiment in two mature forests and estimated annual R_g and R_m. Because experimental conditions in the field are complex, especially in mature natural forests, the uncertainty in partitioning should be large. To decrease the uncertainty, (Cui et al. 2021) conducted an experiment in a young forest regenerating on bare soil in relatively simple conditions resulting from homogeneous tree age, little litter accumulation, limited coarse roots, little ground vegetation, and poor SOM. However, their study's spatial replication was small (n = 10), and R_{ion} was ignored. More field data are indispensable for the robustly parameterization and verification of the partitioning model. Thus, a field experiment was conducted at the same site as (Cui et al. 2021). We increased the number of replications and added R_{ion} as a respiratory component. The objectives of this study were 1) to modify the partitioning model including R_{ion}, 2) to robustly parameterize the modified model using a large size of field data, 3) to quantitatively partition R_r into R_g, R_m, and R_{ion}, and 4) to show the seasonal variations of the R_r components.

2. Material and Methods

2.1. Study site

An experiment was conducted in a young forest in Hokkaido, Japan (42°44.27′N, 141°31.42′E, 116 m above sea level), which was the same site as (Cui et al. 2021). The forest was dominated by Japanese larch (*Larix kaempferi*) and dotted with Japanese white birch (*Betula platyphylla*). The site was used as a mature larch plantation growing on volcanogenous regosol but was severely damaged by a windstorm in 2004 (Sano et al. 2010). All tree stems were removed in 2005. In 2006, a thin layer of organic topsoil

(A horizon), coarse woody debris, stumps, accumulated litter, regenerating ground vegetation, and buried seeds were removed. As a result, volcanic pumice stones (C horizon) were exposed because B horizon was originally lacking. Wind-blown larch seeds germinated in 2007. The ground was sparsely covered with understory species. Aboveground biomass of trees taller than 2 m was 27.3 ± 12.9 and 32.8 ± 9.8 t ha^{-1} (mean ± standard deviation (SD) of three plots of 20 m × 20 m) in September 2019 and September 2020, respectively, of which larch accounted for 82% and 87%, respectively. Belowground biomass of larch coarse roots was 4.50 ± 2.10 and 5.57 ± 1.75 t ha^{-1} in the respective years. Tree biomass was estimated from diameter at breast height (DBH) using allometric equations (Yazaki et al. 2016). Soil bulk density, total carbon (C) and nitrogen (N) concentrations were 0.446 ± 0.042 g cm^{-3}, 15.2 ± 13.8 g kg^{-1}, and 0.742 ± 0.794 g kg^{-1} (mean ±SD, n = 32) for the top 15 cm fine soil layer (< 2 mm) in 2016. Soil C concentration decreased with distance from tree stems, mainly because of decreasing litter fall with distance.

Mean annual air temperature and precipitation were 8.1 ± 0.3°C and 1305 ± 202 mm yr^{-1}, respectively, from 2011 through 2020 at an observatory (Tomakomai) 14 km from the study site. The mean monthly air temperature was highest in August (21.0°C) and lowest in January (-3.9°C). Snow usually covers the ground from early December to early April.

2.2. Experimental design

Nine pairs of aluminum collars (0.5 m × 0.5 m) were concentrically installed 0.5 m and 1.0 m, respectively, from nine isolated larch trees in 50 m × 50 m in July 2019 (Fig. 1). Because root density and root respiration were expected to depend on distances from tree stems, we installed collars at the two positions to ensure a wide range of data. For each pair, collars were positioned at a 0.3–0.4 m interspace and inserted 3 cm deep into the soil. To exclude root respiration, four PVC boards were inserted 30 cm into the soil around the collar (TC) for each pair in July 2019. The soil profiles showed that almost all roots were distributed in the top 15 cm. Fine roots were sampled from the other collar (SC).

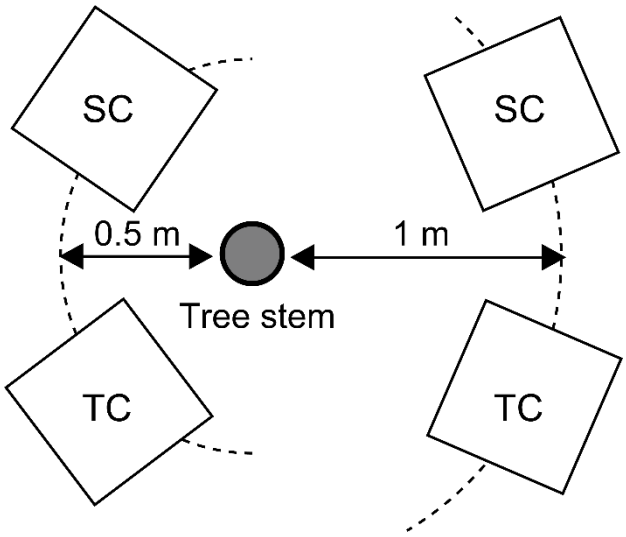

Fig.1. Layout of collars for root sampling (SC) and trenching (TC) 0.5 m and 1.0 m from the tree stem.

2.3. Soil CO_2 flux

Soil CO_2 flux was measured on each collar using a previously described method (Cui et al. 2021; Sun et al. 2017) between 10:00 and 16:00 at intervals of approximately three weeks from August 2019 through November 2020 with a five-month suspension from mid-November 2019 through mid-April 2020. Seedlings were carefully pulled from the collars before flux measurements, although they were rarely found. Flux was measured using a portable system composed of two 0.5-m-tall cubic chambers and a CO_2 analyzer (LI820; Li-Cor Inc., Lincoln, NB, USA). The two chambers were automatically closed for 3 min and opened sequentially. Thus, the flux measurement on the two collars took 6 min. During closing, the CO_2 concentration was measured every 5 s, and its rate of increase was determined using the least-squares method to calculate CO_2 flux. In each collar, soil temperature at a depth of 5 cm and volumetric soil moisture of the top 5 cm were measured immediately after the flux measurement. In addition, soil temperature and soil moisture were recorded half-hourly at depths of 6 cm and 3 cm, respectively, at a station (Hirano et al. 2017) approximately 150 m from the study site.

After trenching, CO_2 flux from the TC (R_{TC}) was equivalent to the sum of the original R_h and additional CO_2 flux resulting from the decomposition of dead roots (R_{DR}) caused by trenching. R_{DR} estimation method is described later. Although the CO_2 flux from the SC (R_{SC}), which was equivalent to the total R_s, was influenced by core sampling, the sampling effect on the CO_2 flux was expected to

139 negligible owing to the limited sampling area (Sun et al. 2020). R_r was estimated for each collar pair as
140 $R_r = R_{SC} - R_{TC} + R_{DR}$ under the assumption that R_h was identical in each pair. Because they were
141 concentrically installed (Fig. 1), SOM and litter fall were assumed to be the same between the two collars
142 in each pair.

143 The following equation was applied to relate the CO_2 flux (R_c, μmol m^{-2} s^{-1}) to soil temperature
144 (T_s, °C) for each collar.

145 $$R_c = a \cdot exp(b \cdot T_s) \quad (1)$$

146 where a and b are the fitting parameters. Using this equation, R_{SC} and R_{TC} were calculated half-hourly
147 from half-hourly soil temperature, and daily R_r was calculated from daily R_{SC}, R_{TC} and R_{DR}.
148

149 **2.4. Decomposition of dead roots**

150 The daily R_{DR} (g C m^{-2} d^{-1}) in TC at elapsed time t (days) was calculated using the following equation
151 for fine and coarse roots, respectively:

152 $$R_{DR} = C_c \cdot (X_{t-1} - X_t) = C_c \cdot X_0 \cdot \exp(-k \cdot t) \cdot \{\exp(k) - 1\} \quad (2)$$

153 where C_c is the C concentration of roots (g g^{-1}), X_t is the dry weight of the remaining dead roots (g m^{-2})
154 at t, X_0 is the initial dry weight of dead roots (g m^{-2}), and k is the decay constant (d^{-1}). X_0 was set for each
155 TC based on the root biomass measured in its paired SC by soil core sampling in September 2019 for
156 fine roots and soil bulk sampling in April 2021 for coarse roots. The root biomass (X_0) was 134 ± 54 at
157 0.5 m and 111 ± 75 g m^{-2} at 1.0 m for fine roots, and 41.6 ± 10.0 at 0.5 m and 18.3 ± 6.3 g m^{-2} at 1.0 m
158 for coarse roots (mean ± SD, n = 9). The diameter of the coarse roots was mostly less than 10 mm with
159 a rough average of 5 mm. The C_c was set separately for fine and coarse roots based on the CN analysis
160 of root samples collected in April 2021; C and N concentrations were 0.455 ± 0.026 g g^{-1} and 9.22 ±
161 0.83 mg g^{-1}, respectively, for fine roots, and 0.489 ± 0.014 g g^{-1} and 7.10 ± 1.25 mg g^{-1}, respectively, for
162 coarse roots (mean ± SD, n = 10). The C and N concentrations differed significantly between fine and
163 coarse roots ($P < 0.01$, two-sided t-test). We used k values determined from litter bag experiments in our
164 previous studies. For fine roots, the k was set at $2.1 \times 10^{-3} \pm 7.4 \times 10^{-4}$ d^{-1} (± standard error (SE)) before
165 mid-November 2019, 0.0 d^{-1} in winter, and $1.7 \times 10^{-3} \pm 4.5 \times 10^{-6}$ d^{-1} after mid-April 2020 (Cui et al.
166 2021), whereas it was set at $6.8 \times 10^{-4} \pm 4.5 \times 10^{-5}$ d^{-1} for coarse roots throughout the period (Sun et al.

2020).

2.5. Biomass and production of fine roots

The same method as in (Cui et al. 2021) was applied to measure fine root biomass and production. Biomass density (B_f, g m^{-2}) was determined by soil coring eight times from September 2019 through November 2020 with a suspension for five months in winter. Soil cores were collected down to 15 cm using a stainless-steel edged tube with an inner diameter of 2.4 cm. Three cores were collected from randomly selected single-use grid positions with an 8 cm spacing in each SC. The area of pits caused by core sampling came to 109 cm^2 in total for each SC (= 4.52 cm^2 × 3 positions × 8 times), accounting for 4.3% of the collar area (0.5 m × 0.5 m). Core samples were stored in PVC tubes in a freezer. Living fine roots were visually extracted from the soil samples dispersed in tap water, dried at 70°C for 48 h, and weighed to determine biomass.

The ingrowth core method was applied to measure production (P_f, g m^{-2} $period^{-1}$). Plastic hair curlers with an outer diameter of 2.3 cm were wrapped in a 2 mm mesh fabric and filled with air-dried root-free soil. The soil was collected from the study site and sieved through 2 mm meshes. In each SC, three ingrowth cores were inserted down to 15 cm into the pit dug through soil core sampling, and the three ingrowth cores installed the previous time were collected. Fine root biomass in the cores, corresponding to root production during the interval, was analyzed using the same method as described above. In addition, annual mortality (M_f, g m^{-2} yr^{-1}) were estimated by subtracting the annual difference in root biomass (ΔB_f) from annual production ($M_f = P_f - \Delta B_f$). The dry weight was converted to C by using C_c (0.455 g g^{-1}). In addition, turnover rates were determined by dividing the annual production by the mean biomass (Brunner et al. 2013).

2.6. Sap flow

The sap flow was measured to quantify ion uptake respiration (R_{ion}). In laboratory experiments, R_{ion} was usually correlated with N uptake as a major nutrient ion, as determined by destructive sampling (Lambers et al. 2008). However, applying this method to trees is difficult in the field because the N analysis of whole trees is expensive and labor-intensive. It was reported that N uptake depends on root

water uptake, causing water mass flow in the soil, especially when root density is low (Henriksson et al. 2021; McMurtrie and Nasholm 2018; Oyewole et al. 2014). We adopted the sap flow rate as a proxy for water uptake and incorporate it into the partitioning model described below.

Sap flow velocity was measured using the thermal dispersion method (Granier 1987) in three trees form July 2019 through November 2020 with a suspension during the leafless season. Sap flow sensors (CUP-SPF-M; Climatec Inc., Tokyo, Japan) were installed 25 cm below the lowest branch to measure the entire sap flow of each tree. From the destructive sampling, we presumed that the stem area at the sensor height (25–72 cm^2) was occupies by sapwood, excluding bark. Thus, sap flow rates were calculated as the product of the sap flow velocity and the stem area. Although sap flow, transpiration, and water uptake were not the same, their daily rates were almost identical. Because DBH of larch trees averaged 54.4 ± 28.3 mm in 2019 (n = 215) and 58.2 ± 30.4 mm in 2020 (n = 225) in the study site, the three trees with DBH of 37–84 mm in 2019 and 43–91 mm in 2020 were almost within the range of mean ± SD in size. The total coarse root biomass of each sample tree was estimated from the DBH using an allometric equation, and the total fine root biomass of each tree was estimated from the coarse root biomass using a factor of 0.185, which was determined from boreal trees (Yuan and Chen 2010). Specific sap flow rates normalized by fine root biomass (S_s; g H_2O g dry matter $(DM)^{-1}$ d^{-1}) were calculated for each tree and averaged. The water uptake rate in each SC was estimated as a product of the average S_s and fine root biomass.

2.7. Partitioning of root respiration

R_r can be partitioned into R_g, R_m, and R_{ion} using the conceptual model below (Amthor 2000; Lambers et al. 2008; Thornley 1970).

$$R_r = R_g + R_m + R_{ion} = g \cdot P_f + m \cdot B_f + u \cdot U_i \quad (3)$$

where g, m, and u are the coefficients of growth, maintenance, and ion uptake respiration, and U_i is the ion uptake rate. Considering the field conditions, we modified the model, including one without R_{ion} to be consistent with our previous study (Cui et al. 2021), as follows.

$$R_r = R_g + R_m + R_{ion} = g \cdot P_f + d \cdot exp(f \cdot T_s) \cdot \left(B_f + B_c\right) + u \cdot S_s \cdot B_f \text{: Model 1} \quad (4)$$

$$R_r = R_g + R_m = g \cdot P_f + d \cdot exp(f \cdot T_s) \cdot (B_f + B_c)$$: Model 2 (5)

where g is the growth coefficient (g C g DM^{-1}), d is the R_m of the unit biomass at 0°C (g C g DM^{-1} d^{-1}), f is the temperature coefficient ($°C^{-1}$), B_c is the coarse root biomass (g m^{-2}), and u is the ion uptake coefficient (g C g H_2O^{-1}). Although respiration components and root production were originally expressed per unit root biomass, they are per unit ground area here, because respiration per area is easier to measure in the field and more useful to quantify ecosystem carbon cycles. In these models, temperature affects only R_m exponentially (Moyano et al. 2009; Thornley 2011). Although the tree survey indicated coarse root growth during the study period, the growth was ignored in R_g because of the lack of data. However, coarse root biomass was incorporated into R_m based on the assumption that the temperature responses of fine and coarse roots were the same. A nonlinear mixed-effects model was applied to the time-series (eight times) datasets for 18 pairs ($n = 8 \times 18$) to parameterize the models. The data preparation for the parametrization is summarized in Fig. 2. Fine root production was measured eight times and converted into daily values using the day length of the measurement intervals. Fine root biomass was the average of two consecutive measurements at the beginning and end of each interval. Soil temperature and specific sap flow are the mean values of the interval. Coarse root biomass was set to a fixed value measured in April 2021 for each pair.

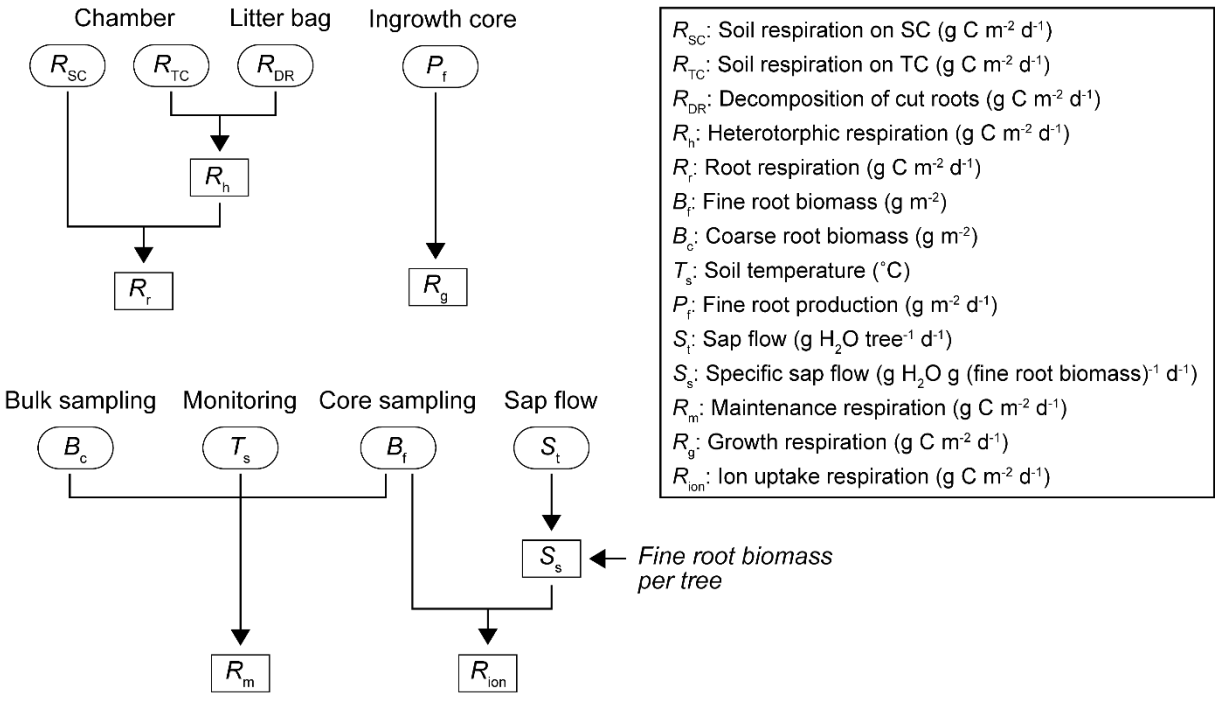

240 **Fig. 2.** Workflow of data preparation for model parameterization.

241

242 **2.8. Data analysis**

243 Student's *t*-test was applied to compare two means, assuming homoscedasticity. Two-way repeated
244 measures analysis of variance (ANOVA) was used to test the effects of factors. For the mixed-effects
245 model application, we used the package 'nlme' in R (Pinheiro et al. 2022). Uncertainties (SD) in the
246 annual summation of respiration components due to model parameterization (Eqs. 1, 2, 4 and 5) were
247 determined by a bootstrap approach (n = 1000), in which model parameters were randomly generated
248 according to a normal distribution with the mean ± SE of each parameter. The uncertainties were
249 propagated by the law of error propagation. Finally, the uncertainties due to parameterization and spatial
250 variation were combined (combined SD) at 0.5 m and 1.0 m, respectively.

251

252 **3. Results**

253 **3.1. Environmental conditions**

254 The field experiment was conducted from September 2019 through November 2020. In the annual
255 period from October 2019 to September 2020, the mean air temperature was 8.6°C, which was higher
256 than its decadal mean + 1 SD, whereas the total precipitation of 1168 mm was within the range. The
257 five-day moving average of soil temperature broadly peaked at 22–23°C from early August to mid-
258 September and was below -1°C from late December to mid-February, with a negative peak at -3°C in
259 mid-January (Fig. 3a). Soil moisture fluctuated between 0.1 and 0.2 m^3 m^{-3} in the snowless season
260 mainly according to precipitation but rapidly decreased in December by soil freezing and then gradually
261 increased under snow accumulation because of the thawing of frozen soil (Fig. 3b). Sap flow showed a
262 seasonal pattern like temperature seasonality but with a large fluctuation mainly due to variable solar
263 radiation (Fig. 3c).

264

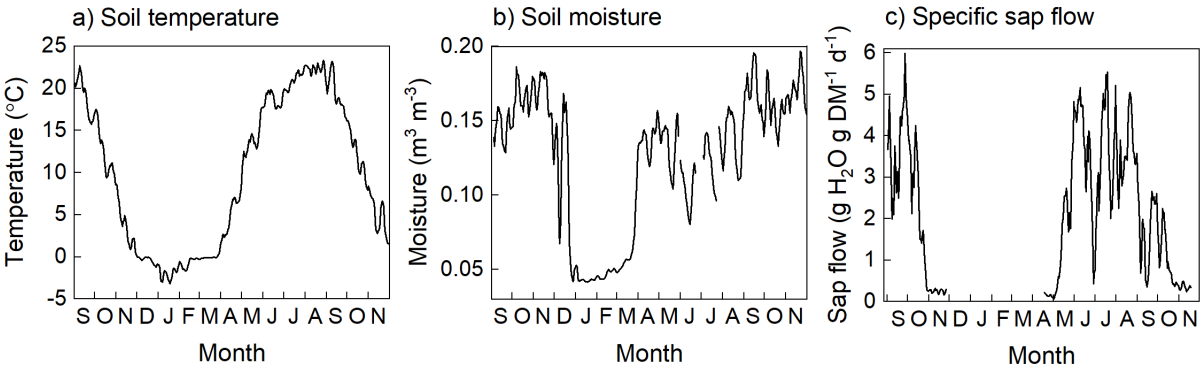

Fig. 3. Seasonal variations in daily means of soil temperature at a depth of 6 cm (a), volumetric soil moisture at a depth of 3 cm (b), and mean specific sap flow (n = 3) (c) from September 2019 to November 2020. Five-day moving averages are shown.

3.2. Soil CO_2 flux

Soil CO_2 flux varied seasonally, following temperature variation (Fig. 4a). Fluxes were 2.54 ± 1.53 (R_{SC}) and 1.44 ± 0.89 (R_{TC}) µmol m^{-2} s^{-1} at 0.5 m and 2.03 ± 1.53 (R_{SC}) and 1.15 ± 0.80 (R_{TC}) µmol m^{-2} s^{-1} at 1.0 m (mean ± SD, n = 135). According to two-way repeated measures ANOVA by setting the date as a block factor, R_{TC} was significantly smaller than R_{SC} at both positions ($P < 0.0001$, $n = 9$). In addition, R_{TC} was smaller than R_{SC} in each pair, with a few exceptions when R_{SC} was smaller than 1.5 µmol m^{-2} s^{-1}, and a significant correlation was found between the fluxes ($P < 0.0001$) (Fig. 5). Meanwhile, a significant exponential relationship was found between soil CO_2 flux and soil temperature (Eq. 1) on each collar (R^2 = 0.48–0.77, $P < 0.01$). However, no significant linear or curvilinear relationship was found between temperature-normalized fluxes and soil moisture, as in our previous studies (Cui et al. 2021; Sun et al. 2020). Thus, half-hourly R_{SC} and R_{TC} were calculated for each collar from monitoring soil temperature (Fig. 3a), using each exponential equation. Both soil temperature and soil moisture measured in collars did not differ significantly between positions (0.5 m vs. 1.0 m) or treatments (SC vs. TC).

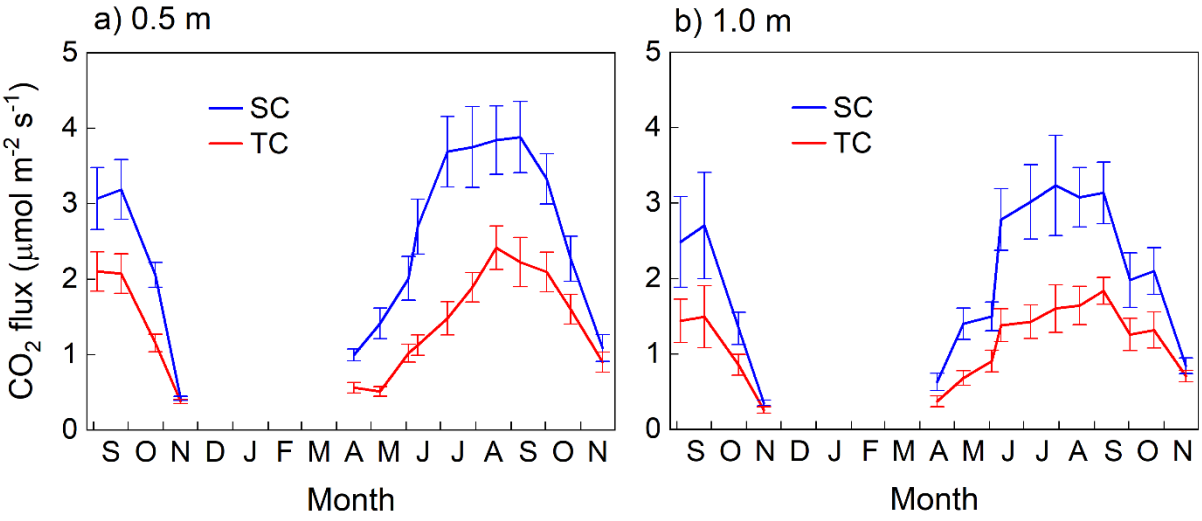

Fig. 4. Seasonal variations in soil CO_2 flux on control collars (SC) and trenched collars (TC) at 0.5 m (a) and 1.0 m (b) from September 2019 to November 2020. Vertical bars denote standard errors (n = 9).

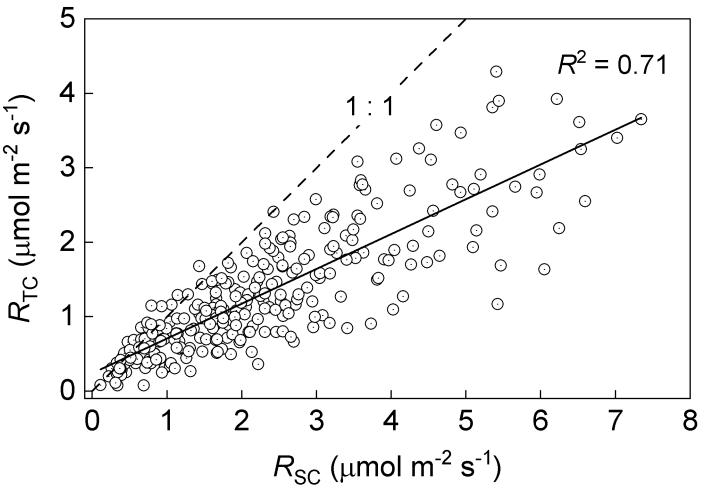

Fig. 5. Relationship between soil CO_2 fluxes measured in trenched collars (R_{TC}) and control collars (R_{SC}) of each pair. The dashed line denotes a 1:1 relationship. The solid line denotes liner regression.

In each pair of collars, daily soil respiration ($R_s = R_{SC}$) was partitioned into R_h and R_r. R_s, R_r, and R_h varied similarly to the seasonal pattern of soil temperature, because both R_{SC} and R_{TC} were calculated from soil temperature (Figs. 6a and 6b). In addition, the contribution of R_r to R_s (R_r / R_s) showed a clear seasonal variation (Fig. 6c). The R_r / R_s decreased sharply during the fall until late November and continued decreasing to 0.36–0.37 until late March under snow accumulation. After snow disappearance

in April, R_r / R_s rapidly increased and reached a broad peak of approximately 0.5 in summer from late June to early September 2020.

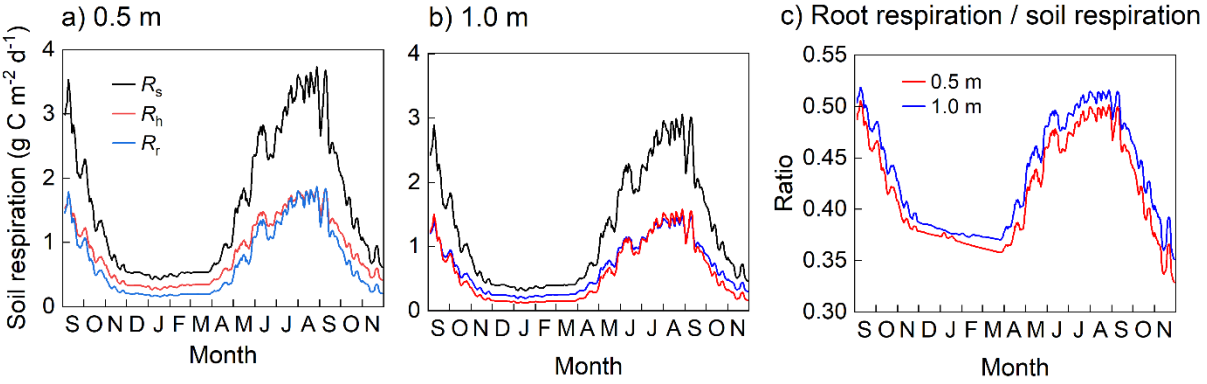

Fig. 6. Seasonal variations in mean daily soil respiration (R_s), heterotrophic respiration (R_h) and root respiration (R_r) at 0.5 m (a) and 1.0 m (b), and the ratio of root respiration and soil respiration (c) (n =9) from September 2019 to November 2020. Five-day moving averages are shown.

Annually, R_s was partitioned into R_h and R_r by 55% vs. 45% at 0.5 m and 53% vs. 47% at 1.0 m (Table 1). The CO_2 emissions through dead root decomposition (R_{DR_all}) accounted for 5.9% and 4.5% of R_s at 0.5 m and 1.0 m, respectively.

Table 1. Annual soil CO_2 fluxes (g C m^{-2} yr^{-1}) (mean ± combined standard deviation).

Position	R_{SC} (R_s)	R_{TC}	R_{DR_f}	R_{DR_c}	R_{DR_all}	R_h	R_r
0.5 m	562 ± 123 (100)	341 ± 100 (61)	27 ± 16 (4.8)	6 ± 3 (1.1)	33 ± 16 (5.9)	308 ± 101 (55)	253 ± 159 (45)
1.0 m	447 ± 107 (100)	256 ± 74 (57)	17 ± 21 (3.8)	3 ± 2 (0.7)	20 ± 21 (4.5)	237 ± 77 (53)	210 ± 132 (47)

1) R_{SC} (R_s): soil CO_2 flux in the sampling collar (SC) or total soil respiration, R_{TC}: soil CO_2 flux in trenched collars (TC), R_{DR_f}: CO_2 emissions through the decomposition of dead fine roots, R_{DR_c}: CO_2 emissions through the decomposition of dead coarse roots, R_{DR_all}: the sum of R_{DR_f} and R_{DR_c}: R_h: heterotrophic respiration, R_r: root respiration

2) The numbers in parentheses denote the percentages of R_{SC} at each position. The annual value was calculated as the average of the sums for the two annual periods, i.e., October 2019 through September 2020 and November 2019 through October 2020.

3.3. Biomass and production of fine roots

Seasonal variation in fine root biomass was ambiguous, despite a small peak in early summer (Fig. 7). In contrast, fine root production showed a clear seasonal pattern (Fig. 8), with a peak in June to July. In the cold season from mid-November thorough mid-April, root production was small at 0.11 ± 0.005 and 0.12 ± 0.069 g m^{-2} d^{-1} (mean ± SE) at 0.5 m and 1.0 m, respectively. Annual values were shown in Table 2. Only the turnover rates were significantly different between the two positions ($P < 0.05$).

To compare the spatial variation of biomass and production between two scales of the collar (0.5 m × 0.5 m) and the study area (50 m × 50 m), the standard deviations (SDs) of biomass and production measured at three points within each SC were calculated and averaged for nine locations at 0.5 m and 1.0 m, respectively, for each sampling date. For all sampling dates ($n = 8$), the mean ± SD values of the averaged SD (within collar) were 47.2 ± 5.7 (0.5 m) and 37.9 ± 6.2 (1.0 m) g m^{-2} for biomass, and 0.249 ± 0.155 (0.5 m) and 0.229 ± 0.130 (1.0 m) g m^{-2} d^{-1} for production. Meanwhile, the SD of the mean biomass and production from nine individual locations (within study area) was calculated and averaged for all sampling dates to be 76.6 ± 14.4 (0.5 m) and 73.6 ± 23.8 (1.0 m) g m^{-2} for biomass, and 0.363 ± 0.210 (0.5 m) and 0.309 ± 0.190 (1.0 m) g m^{-2} d^{-1} for production. Spatial variation expressed by the mean SD was smaller within the collar than within the study area by 40–50% for biomass and 25–50% for production.

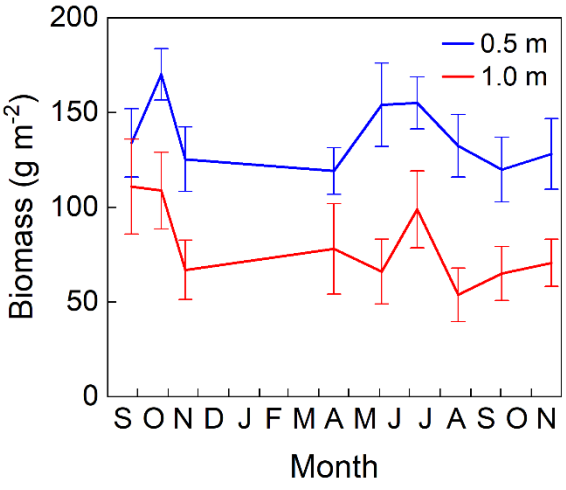

Fig. 7. Seasonal variation in fine root biomass at 0.5 m and 1.0 m ($n = 9$) from September 2019 to November 2020. Means (± standard errors) were shown.

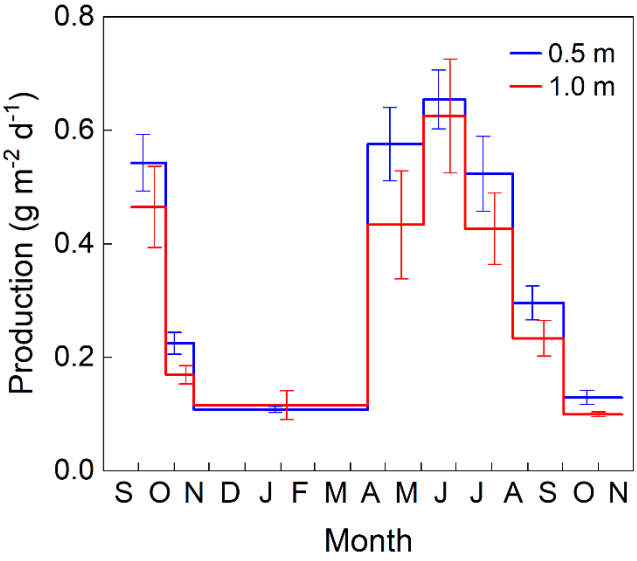

342

343 **Fig. 8.** Seasonal variation in fine root production at 0.5 m and 1.0 m (n = 9) from September 2019 to
344 November 2020. Means (± standard errors) were shown.

345

346 **Table 2.** Annual fine root dynamics (mean ± standard deviation, n = 9).

Position	P_f (g m^{-2} yr^{-1})	ΔB_f (g m^{-2} yr^{-1})	M_f (g m^{-2} yr^{-1})	Mean B_f (g m^{-2})	Turnover rate (yr^{-1})*	Mean B_c (g m^{-2})
0.5 m	116 ± 19	3 ± 48	113 ± 99	133 ± 40	0.90 ± 0.30	44 ± 42
1.0 m	103 ± 29	4 ± 26	98 ± 39	78 ± 43	1.68 ± 0.84	20 ± 26

347 * $P < 0.05$, between positions by two-sided t test
348 1) P_f: fine root production, ΔB_f: annual difference in fine root biomass, M_f: fine root mortality, B_f: fine
349 root biomass, B_c: coarse root biomass
350 2) The annual value was calculated as the average of the sums for the two annual periods, i.e., October
351 2019 through September 2020 and November 2019 through October 2020.
352

353 **3.4. Partitioning of root respiration**

354 Both models (Eqs. 4 and 5) were significantly parameterized using the dataset ($P < 0.0001$, R^2 =
355 0.57–0.59) (Table 3). All parameters were determined to be statistically significant ($P < 0.012$).
356 Parameter d, the maitenance respiration of the unit biomass at 0°C, was almost identical in the two
357 models. The Q_{10} values calculated from the parameter f were 2.34 and 2.61 in Models 1 and 2,
358 respectively. $d \cdot exp(f \cdot T_s)$ in the models, corresponding to the maintenance respiration coefficient (m) in
359 Eq. 3, was 0.0013 at 5°C, 0.0030 at 15°C, and 0.0070 g C g DM^{-1} d^{-1} at 25°C in Model 1 and 0.0013 at

5°C, 0.0034 at 15°C, and 0.0089 g C g DM^{-1} d^{-1} at 25°C in Model 2. The coefficients were the same at 5°C across the models, but 12% and 21% lower in Model 1 at 15°C and 25°C, respectively, because of a lower temperature coefficient. In addition, the coefficient of growth respiration (*g*) was 22% lower in Model 1. The decreases in *f* and *g* in Model 1 were compensated for by the coefficient of ion uptake respiration (*u*).

Table 3. Model parameters (± standard error).

	Model 1		Model 2	
	Parameter	*P*	Parameter	*P*
Growth respiration coefficient (*g*) (g C g DM^{-1})	0.57 ± 0.14	0.0001	0.73 ± 0.13	< 0.0001
Maintenance respiration coefficient at 0°C (*d*) (g C g DM^{-1} d^{-1})	0.00084 ± 0.00027	0.0019	0.00081 ± 0.00025	0.0015
Temperature coefficient (*f*) ($°C^{-1}$)	0.085 ± 0.015	< 0.0001	0.096 ± 0.014	< 0.0001
Ion uptake respiration coefficient (*u*) (g C g H_2O^{-1})	0.00045 ± 0.00018	0.012		
Adjusted R^2	0.59		0.57	
P	< 0.0001		< 0.0001	

Annual R_r was partitioned into fine root R_g, fine root R_m (R_{m_f}) and coarse root R_m (R_{m_c}), and R_{ion} using the fitting parameters (Table 4). The results from the models were overestimated by 7% at 0.5 m and underestimated by 10% at 1.0 m in total (Sum / R_r). R_{m_f} contributed the most to R_r (46–51%), followed by R_g (26–40%). R_g, R_{m_f}, and R_{m_c} were smaller in Model 1 by 19, 8, and 5 g C m^{-2} yr^{-1}, respectively, at 0.5 m and by 16, 5, and 2 g C m^{-2} yr^{-1}, respectively, at 1.0 m. R_g showed the largest difference between the two models, suggesting that the majority of R_{ion} was lumped together with R_g in Model 2. Fine root R_r (Sum – R_{m_c}) accounted for 86–90% and 84–89% of the total R_r (Sum) in Models 1 and Model 2, respectively.

Table 4. Annual sums of root respiration components (g C m^{-2} yr^{-1}) (mean ± combined standard deviation).

Model 1

Position	R_r	R_g	R_{m_f}	R_{m_c}	R_{ion}	Sum
0.5 m	253 ± 227 (93)	70 ± 23 (26)	130 ± 66 (48)	39 ± 45 (14)	32 ± 17 (12)	271 ± 93 (100)

1.0 m	210 ± 151 (112)	60 ± 32 (32)	87 ± 74 (46)	18 ± 44 (10)	23 ± 17 (12)	188 ± 122 (100)

Model 2

Position	R_r	R_g	R_{m_f}	R_{m_c}	Sum
0.5 m	253 ± 227 (93)	89 ± 25 (33)	138 ± 76 (51)	44 ± 51 (16)	271 ± 99 (100)
1.0 m	210 ± 151 (112)	76 ± 39 (40)	92 ± 83 (49)	20 ± 49 (11)	188 ± 124 (100)

1) R_r: root respiration (from Table 2), R_g: growth respiration, R_{m_f}: fine root maintenance respiration, R_{m_c}: coarse root maintenance respiration, R_{ion}: ion uptake respiration, Sum: $R_g + R_{m\_f} + R_{m\_c} + R_{ion}$ (Model 1) or $R_g + R_{m\_f} + R_{m\_c}$ (Model 2)

2) The numbers in parentheses denote percentages of the sum. The annual value was calculated as the average of the sums for the two annual periods, e.g., October 2019 to September 2020 and November 2019 to October 2020.

The respiration components varied seasonally with different peak periods. Even though Fig. 9 shows the result at 0.5 m, the seasonal variation was similar at 1.0 m. R_g peaked from June to July in proportion to root production (Fig. 8), whereas R_{m_f} peaked from July to August owing to its positive relationship with soil temperature (Fig. 3a) and fine root biomass (Fig. 7). In addition, R_{m_c} peaked following the temperature variation under the assumption of no seasonality in coarse root biomass. R_{ion} peaked from July to August according to the seasonality of fine root biomass and sap flow (Fig. 3c) and was zero in winter because of defoliation. The relative contribution of each respiration component to R_r also showed seasonality (Figs. 9c and 9d). Seasonal variation in R_g contribution was relatively large, with a peak from April to May at 0.40 (Model 1) and 0.49 (Model 2) and reached a minimum of 0.16 (Model 1) and 0.20 (Model 2) from August to September.

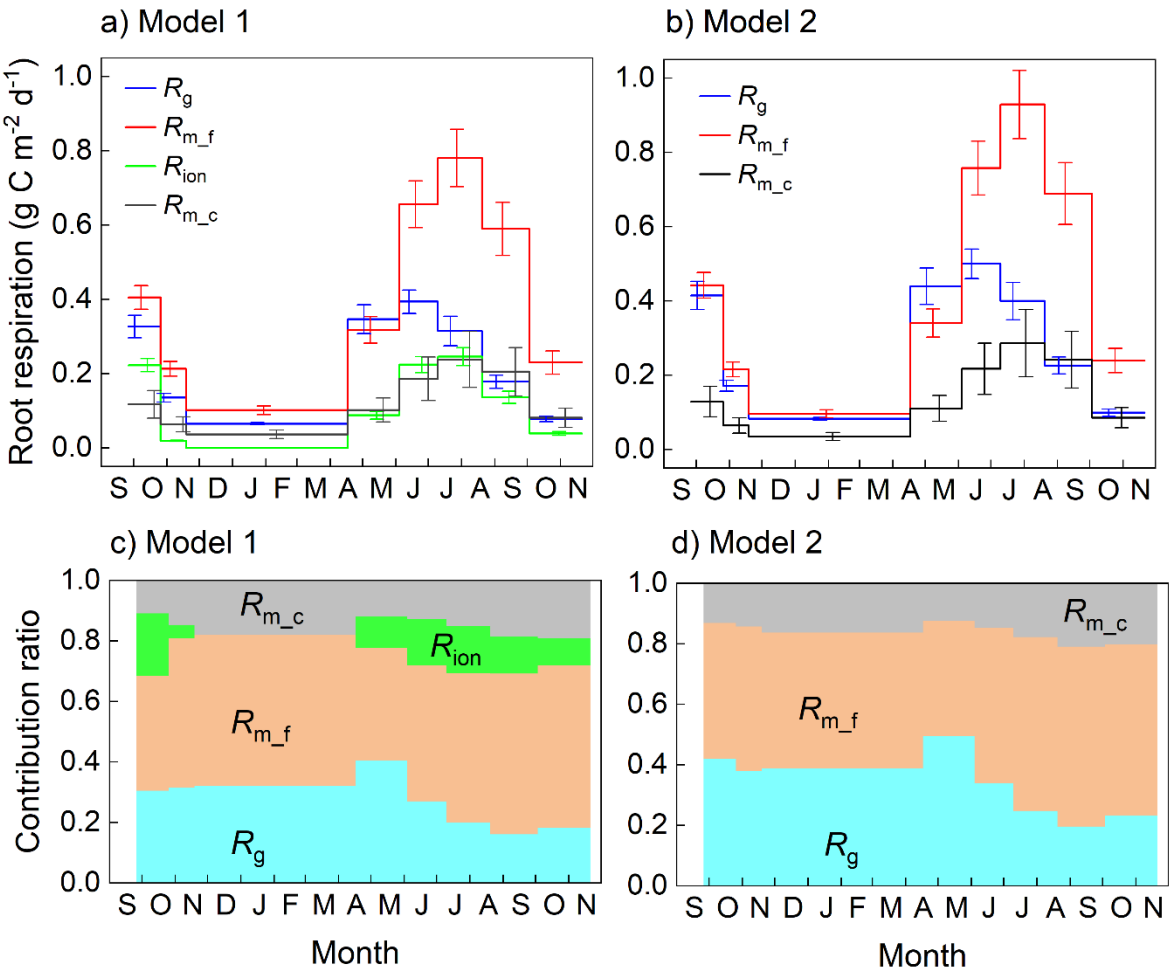

Fig. 9. Seasonal variations in fine root growth respiration (R_g), fine root maintenance respiration (R_{m_f}), coarse root maintenance respiration (R_{m_c}), and ion uptake respiration (R_{ion}) at 0.5 m estimated by Model 1 (a) and Model 2 (b) from September 2019 to November 2020. Means (± standard errors, n = 9) were shown. Contribution ratios of the respiration components from Model 1 (c) and Model 2 (d) are also shown.

4. Discussion

4.1. Partitioning of soil respiration

The CO_2 emission (R_{DR}) from the decomposition of dead roots caused by trenching was estimated using the decay constant from root litterbag experiments, which were reported to underestimate fine root decomposition by 10–20% because of rhizosphere disturbance (Dornbush et al. 2002). However, the effect of the underestimation would be limited, because annual fine root decomposition was small, accounting for 4–5% of total soil respiration (Table 1). Meanwhile, trenching would have decreased R_h

because of the lack of litter supply from the living roots. In addition, no priming effect of labile exudate from roots on microbial decomposition was expected (Kuzyakov 2010). Thus, R_h was potentially underestimated, although the underestimation could have been limited because of low root density, which was much lower at 78–133 g m^{-2} (Table 2) than the average density (505 g m^{-2}) of temperate deciduous forests (Finér et al. 2011a). Although soil moisture was expected to increase in TC because of no water uptake by roots (Subke et al. 2006), there was no difference between SC and TC, probably because of the low root density.

Periodically measured CO_2 fluxes were extrapolated to sequential data for each collar using an exponential equation (Eq. 1) from the continuously measured soil temperature. It is common to determine representative R_h and R_r values from the spatial averages of soil CO_2 fluxes in a study area because of their large spatial variations (Sun et al. 2020). However, we determined R_h and R_r in each pair of collars to ensure the spatial variation of R_r based on the assumption that R_h values on the two collars (SC and TC) in each pair were similar. The assumption was because the two collars were closely installed (0.3–0.4 m apart) and equally distant from each isolated larch stem, suggesting that SOM, leaf litter accumulation, and root density were at a similar level in the two neighboring collars. We confirmed that soil CO_2 fluxes in the two collars were similar before trenching, and soil C concentration decreased with increasing distance from tree stems (Cui et al. 2021). The significant linear relationship between R_{TC} and R_{SC} (Fig. 4) supports this assumption. In addition, the result that spatial variation in fine root biomass was considerably smaller on a collar scale than on the scale of the study area suggests a similar soil condition in each collar pair.

Compared to our previous study conducted two years ago (Cui et al. 2021), annual R_h slightly decreased by 2% at 0.5 m and 9% at 1.0 m, but annual R_r increased by 40% at 0.5 m and 412% at 1.0 m. The R_r increase was due to tree growth; fine root biomass increased twofold at 0.5 m and sixfold at 1.0 m in two years (Table 2). The annual contribution of R_r to R_s was 45–47% (Table 1), which is comparable to the results of meta-analyses (Hanson et al. 2000; Subke et al. 2006).

4.2 Partitioning of root respiration

Soil CO_2 flux and fine root dynamics were simultaneously measured within the same collar (SC) to

minimize spatial mismatches. Although soil core sampling disturbed soil conditions, the disturbance would be insignificant to CO_2 flux (Sun et al. 2020) because the total pit area caused by eight-time core samplings was only 4.3% in each SC, and sampling intervals were more than a month.

We applied the ingrowth core method to measure root production. The method tends to underestimate root production compared to the minirhizotron method which potentially yields more reliable estimates (Addo-Danso et al. 2016; Finér et al. 2011b; Hendricks et al. 2006). The annual fine root production was 103–116 g m^{-2} yr^{-1} in this study (Table 2), which was much smaller than the average (337 g m^{-2} yr^{-1}) of temperate forests (Finér et al. 2011b). However, turnover rates (0.90–1.68 yr^{-1}, Table 2) were comparable to those of temperate forests (Brunner et al. 2013; Finér et al. 2011b). Thus, our results might not have been underestimated, because ingrowth cores were sampled at relatively short intervals of 5–7 weeks using thinner cores with a diameter of 2.3 cm. Short intervals probably enhanced root production in conditions of low root competition and less decomposition, and thin cores could minimize the delayed root recolonization (Hertel and Leuschner 2002; Li et al. 2013).

All parameters were significantly determined in the models, whereas the models explained R_r variations by only 57–59% (Table 3). We excluded coarse root growth from R_g. (Wieser and Bahn 2004) reported that R_m of coarse roots (R_{m_c}) accounted for 73–83% of total coarse root respiration. Accordingly, coarse root growth respiration was roughly estimated from R_{m_c} (Table 4) to be 8–12 g C m^{-2} yr^{-1} at 0.5 m and 4–5 g C m^{-2} yr^{-1} at 1.0 m, which accounted for 3–4% and 2–3% of total R_r, respectively. In addition, we set coarse root biomass at the measurements in April 2021 after the experiment, ignoring its phenological variation. Coarse root biomass would have increased during the growing season because tree surveys indicated an annual growth in the study site from 2019 to 2020. Thus, the root biomass in April 2021 would be close to the maximum for the experimental period, and consequently, R_{m_c} was probably overestimated to some extent. The parameters related to R_m (d and f) were common for fine and coarse roots in the models to make the model simpler and nonlinear fitting converge. However, the parameters might be smaller for coarse roots, because N concentration was significantly lower in coarse roots than in fine roots (7.10 ± 1.25 vs. 9.22 ± 0.83 mg g^{-1}); R_m is positively related to protein content (Lambers et al. 2008). Because trenching was conducted using PVC boards, calculated R_r consists of respiration by roots alone and rhizomicrobial and mycorrhizal respirations

(Moyano et al. 2009). Rhizomicrobial and mycorrhizal respirations were not incorporated in the models. However, these respirations were probably stimulated by the translocation of photosynthate to roots, depending on root-derived compounds. Therefore, rhizomicrobial and mycorrhizal respirations should be included in R_g estimated from root production. In a mature Japanese larch forest, the contribution of respiration by roots plus rhizomicrobial respiration to R_s and mycorrhizal respiration to R_s were 42% and 6%, respectively, during the growing season (Makita et al. 2021).

The annual partitioning of R_r to four (Model 1) or three components (Model 2) at 0.5 m and 1.0 m were similar (Table 4), although the absolute values were smaller at 1.0 m. R_{m_f} accounted for the majority (46–51%), followed by R_g (26–40%) and R_{m_c} (10–16%) or R_{ion} (12%). In comparison between the two models, the largest difference was found in R_g, suggesting that the majority of R_{ion} was lumped together with R_g when R_{ion} was not considered, which is supported by the strong correlation between plant growth and ion uptake (Lambers et al. 2008).

Fine root growth even in the snow season (Radville et al. 2016) was suggested by ingrowth core sampling in mid-April (Fig. 8). Thus, relatively high contribution of R_g to R_r was possible during winter (Fig. 9). However, the root production measured in mid-April may have resulted from rapid growth after snow disappearance in early April (Fig. 3a) (McCormack et al. 2015b). The contribution of R_g showed a clear seasonal variation, with a small peak in mid-spring and a minimum in early fall, because of the time lag of seasonal variation between fine root production (Fig. 8) and soil temperature (Fig. 3a). R_g exceeded R_{m_f} only in mid-spring. Although R_g and R_{m_f} were larger in this study compared to our previous study (Cui et al. 2021) because of large increase in fine root production and biomass in two years, the annual contribution ratios of R_g, R_{m_f}, and R_{m_c} to R_r was unchanged at 0.5 m. However, the results of this study (Table 4) were much different from those of a field study in evergreen and deciduous plantations (George et al. 2003), in which fine root R_m accounted for 86–92% of R_r and the contribution of R_{ion} was only 4%. The difference is mainly attributable to different methods as described below.

The coefficients of Models 1 and 2 are compared with those from other studies (Table 5). To convert the unit of O_2 to C of CO_2, the respiration quotient was assumed to be one. Compared with (Cui et al. 2021), the g for growth respiration of the same model (Model 2) rose by 26% in this study, whereas the m for maintenance respiration was almost the same. Although R^2 was almost the same, the standard

errors of the parameters (*g*, *d*, and *f*) were smaller in this study (Table 3) mainly because of more replications. This and our previous studies (Cui et al. 2021; Sun et al. 2020) showed a larger *g* than those of the other tree species (*Quercus suber*, *Ecualyptus* sp., *Pinus Taeda*, and *Liquidambar styraciflua*) The difference is mainly due to different methods and different experimental conditions. For *Quercus suber* and *Ecualyptus* sp., the *g* for all roots, including coarse roots, was determined from relative growth rates of hydroponically cultured seedlings or cuttings in a controlled environment (Lambers et al. 2008; Thongo M'Bou et al. 2010). In addition, the fine root *g* for *Pinus taeda* and *Liquidambar styraciflua* was determined from a laboratory calorimetric experiment (George et al. 2003). The carbon cost of producing new root biomass was reported to be 0.536 g C g DM^{-1} on average (Chapin et al. 2011; Poorter 1994). From the carbon cost, carbon consumed through growth respiration was roughly estimated to be 0.11 g C g DM^{-1} under the assumption that respiration cost accounts for 20% of the total cost (Chapin et al. 2011). Our *g* derived from field experiments were consistently higher than the respiration cost from laboratory experiments. The large difference in *g* suggests that more energy is necessary for fine root production in the field. In contrast, the *m* was relatively stable among tree species, except for smaller *m* for mature spruce.

Table 5. Comparison of model parameters.

Plant species	Experiment	Growth respiration coefficient (*g*) (g C g DM^{-1})	Maintenance respiration coefficient (*m*) (mg C g DM^{-1} d^{-1})	Temperature (°C)	Ion Uptake respiration (R_{ion})	Reference
Dactylis glomerta	Laboratory	0.13	27	No data	No	Lambers *et al.*, 2008
Festuca ovina		0.23	22			
Quercus suber		0.14	6.2			
Triticum aestivum		0.22	23			
Eucalyptus sp.	Greenhouse	0.06	10	22	No	Thongo M'Bou *et al.*, 2010
Pinus taeda	Forest	0.061	9.2	25	Yes	George *et al.*, 2003
Liquidambar styraciflua		0.070	11			
Mature larch	Forest	0.32	5.7	22	No	Sun *et al.*, 2020
			8.2	25		
Mature spruce		0.24	2.8	22		
			3.7	25		

Young larch	Forest	0.58	6.8	22	No	Cui *et al.*, 2021
			8.1	25		
Young larch	Forest	0.57	5.5	22	Yes	This study (Model 1)
			7.0	25		
Young larch	Forest	0.73	6.7	22	No	This study (Model 2)
			8.9	25		

512

513 We conducted a year-round experiment by increasing spatial replication and incorporating R_{ion} in a
514 young larch-dominated forest regrowing on bare ground. The experimental conditions were
515 considerably simplified because of an almost pure stand, the same tree age, low tree density, little ground
516 vegetation, little litter accumulation, and a small amount of SOM. From the experiments in this study
517 and (Cui et al. 2021), we derived similar parameters (g, d, and f) for partitioning. The Q_{10} of maintenance
518 respiration (2.33–2.61) was reasonable. Therefore, we believe that root respiration was partitioned with
519 a certain level of reliability and the approach was robust under relatively simple conditions. However,
520 we should note that our results were yielded in an unnaturally simple field condition, because the soil
521 without the organic layer was not typical among forest soils. Moreover, our growth respiration parameter
522 (g) resulting from only field data was much higher than those from laboratory experiments. To further
523 improve our understanding of root respiration in the field, more experimental data should be
524 accumulated.

525

526 **Acknowledgement**

527 We thank the Hokkaido Regional Office of the Forestry Agency for allowing us to use the study
528 site, N. Saigusa, Y. Takahashi, R. Hirata and the staff of CGER for managing the site, and K. Ishikura
529 for sharing an R script for the nonlinear mixed effect model.

530

531 **References**

532

533 Abramoff RZ, Finzi AC (2015) Are above- and below-ground phenology in sync? New Phytol 205: 1054-
534 1061. doi: 10.1111/nph.13111.
535 Addo-Danso SD, Prescott CE, Smith AR (2016) Methods for estimating root biomass and production in

536 forest and woodland ecosystem carbon studies: A review. Forest Ecology and Management 359:
537 332-351. doi: 10.1016/j.foreco.2015.08.015.
538 Amthor J (2000) The McCree–de Wit–Penning de Vries–Thornley Respiration Paradigms: 30 Years
539 Later. Ann Bot-London 86: 1-20. doi: 10.1006/anbo.2000.1175.
540 Ballantyne A, Smith W, Anderegg W, Kauppi P, Sarmiento J, Tans P, Shevliakova E, Pan Y, Poulter B,
541 Anav A, Friedlingstein P, Houghton R, Running S (2017) Accelerating net terrestrial carbon
542 uptake during the warming hiatus due to reduced respiration. Nature Climate Change 7: 148-
543 152. doi: 10.1038/nclimate3204.
544 Boone RD, Nadelhoffer KJ, Canary JD, Kaye JP (1998) Roots exert a strong influence on the temperature
545 sensitivity of soil respiration. Nature 396: 570-572.
546 Brunner I, Bakker MR, Björk RG, Hirano Y, Lukac M, Aranda X, Børja I, Eldhuset TD, Helmisaari HS,
547 Jourdan C, Konôpka B, López BC, Miguel Pérez C, Persson H, Ostonen I (2013) Fine-root
548 turnover rates of European forests revisited: an analysis of data from sequential coring and
549 ingrowth cores. Plant Soil 362: 357-372. doi: 10.1007/s11104-012-1313-5.
550 Cannell MGR, Thornley JHM (2000) Modeling the components of plant respiration: some guiding
551 principle. Ann Bot-London 85: 45-54.
552 Chapin FSI, Matson PA, Vitousek PM (2011) Plant carbon buddgets. Principle of terrestrial ecosystem
553 eclogoy. 2nd edn. Springer, New York.
554 Collalti A, Tjoelker MG, Hoch G, Makela A, Guidolotti G, Heskel M, Petit G, Ryan MG, Battipaglia G,
555 Matteucci G, Prentice IC (2020) Plant respiration: Controlled by photosynthesis or biomass?
556 Glob Chang Biol 26: 1739-1753. doi: 10.1111/gcb.14857.
557 Cui R, Hirano T, Sun L, Teramoto M, Liang N (2021) Variations in biomass, production and respiration
558 of fine roots in a young larch forest. Journal of Agricultural Meteorology 77: 167-178. doi:
559 10.2480/agrmet.D-20-00049.
560 Dornbush ME, Isenhart TM, Raich JW (2002) Quantifying fine-root deomposition: an alternative to
561 buried litterbags. Ecology 83: 2985-2990.
562 Finér L, Ohashi M, Noguchi K, Hirano Y (2011a) Factors causing variation in fine root biomass in forest
563 ecosystems. Forest Ecology and Management 261: 265-277. doi: 10.1016/j.foreco.2010.10.016.
564 Finér L, Ohashi M, Noguchi K, Hirano Y (2011b) Fine root production and turnover in forest ecosystems
565 in relation to stand and environmental characteristics. Forest Ecology and Management 262:
566 2008-2023. doi: 10.1016/j.foreco.2011.08.042.
567 Friedlingstein P, O'Sullivan M, Jones MW, Andrew RM, Hauck J, Olsen A, Peters GP, Peters W,
568 Pongratz J, Sitch S, Le Quéré C, Canadell JG, Ciais P, Jackson RB, Alin S, Aragão LEOC, Arneth
569 A, Arora V, Bates NR, Becker M, Benoit-Cattin A, Bittig HC, Bopp L, Bultan S, Chandra N,
570 Chevallier F, Chini LP, Evans W, Florentie L, Forster PM, Gasser T, Gehlen M, Gilfillan D,
571 Gkritzalis T, Gregor L, Gruber N, Harris I, Hartung K, Haverd V, Houghton RA, Ilyina T, Jain
572 AK, Joetzjer E, Kadono K, Kato E, Kitidis V, Korsbakken JI, Landschützer P, Lefèvre N, Lenton
573 A, Lienert S, Liu Z, Lombardozzi D, Marland G, Metzl N, Munro DR, Nabel JEMS, Nakaoka S-

574 I, Niwa Y, O'Brien K, Ono T, Palmer PI, Pierrot D, Poulter B, Resplandy L, Robertson E,
575 Rödenbeck C, Schwinger J, Séférian R, Skjelvan I, Smith AJP, Sutton AJ, Tanhua T, Tans PP,
576 Tian H, Tilbrook B, van der Werf G, Vuichard N, Walker AP, Wanninkhof R, Watson AJ, Willis
577 D, Wiltshire AJ, Yuan W, Yue X, Zaehle S (2020) Global Carbon Budget 2020. Earth System
578 Science Data 12: 3269-3340. doi: 10.5194/essd-12-3269-2020.
579 George K, Norby RJ, Hamilton JG, DeLucia EH (2003) Fine-root respiration in a loblolly pine and
580 sweetgum forest growing in elevated CO2. New Phytologist 160: 511-522. doi: 10.1046/j.1469-
581 8137.2003.00911.x.
582 Granier A (1987) Evaluation of transpiration in a Douglas-fir stand by means of sap flow measurements.
583 Tree Physiology 3: 309-320.
584 Hanson PJ, Edwards NT, Gartedn CT, Andrews JA (2000) Separating root and soil microbial
585 contributions to soil respiration: A review of methods and observations. Biogeochemistry 48:
586 114-146.
587 Hendricks JJ, Hendrick RL, Wilson CA, Mitchell RJ, Pecot SD, Guo D (2006) Assessing the patterns and
588 controls of fine root dynamics: an empirical test and methodological review. J Ecol 94: 40-57.
589 doi: 10.1111/j.1365-2745.2005.01067.x.
590 Henriksson N, Lim H, Marshall J, Franklin O, McMurtrie RE, Lutter R, Magh R, Lundmark T, Nasholm
591 T (2021) Tree water uptake enhances nitrogen acquisition in a fertilized boreal forest - but not
592 under nitrogen-poor conditions. New Phytol 232: 113-122. doi: 10.1111/nph.17578.
593 Hertel D, Leuschner C (2002) A comparison of four different fine root production estimates with
594 ecosystem carbon balance data in a *Fagus-Quercus* mixed forest. Plant Soil 239: 237-251.
595 Hirano T, Suzuki K, Hirata R (2017) Energy balance and evapotranspiration changes in a larch forest
596 caused by severe disturbance during an early secondary succession. Agricultural and Forest
597 Meteorology 232: 457-468. doi: 10.1016/j.agrformet.2016.10.003.
598 Hopkins F, Gonzalez-Meler MA, Flower CE, Lynch DJ, Czimczik C, Tang J, Subke JA (2013) Ecosystem-
599 level controls on root-rhizosphere respiration. New Phytol 199: 339-351. doi:
600 10.1111/nph.12271.
601 Johnson IR (1990) Plant respiration in relation to growth, maintenance, ion uptake and nitrogen
602 assimilation. Plant, Cell and Environment 13: 319-328.
603 Kuzyakov Y (2006) Sources of CO2 efflux from soil and review of partitioning methods. Soil Biology and
604 Biochemistry 38: 425-448. doi: 10.1016/j.soilbio.2005.08.020.
605 Kuzyakov Y (2010) Priming effects: Interactions between living and dead organic matter. Soil Biology
606 and Biochemistry 42: 1363-1371. doi: 10.1016/j.soilbio.2010.04.003.
607 Lambers H, Chapin FSI, Pons TL (2008) The role of respiration in plant carbon balance. Plant
608 Physiological Ecology. 2nd edn. Springer, New York.
609 Lavigne MB, Foster RJ, Goodine G (2004) Seasonal and annual changes in soil respiration in relation to
610 soil temperature, water potential and trenching. Tree Physiology 24: 415-424.
611 Li X, Zhu J, Lange H, Han S (2013) A modified ingrowth core method for measuring fine root production,

612 mortality and decomposition in forests. Tree Physiol 33: 18-25. doi: 10.1093/treephys/tps124.
613 Makita N, Fujimoto R, Tamura A (2021) The Contribution of Roots, Mycorrhizal Hyphae, and Soil Free-
614 Living Microbes to Soil Respiration and Its Temperature Sensitivity in a Larch Forest. Forests
615 12. doi: 10.3390/f12101410.
616 McCormack ML, Adams TS, Smithwick EAH, Eissenstat DM (2014) Variability in root production,
617 phenology, and turnove rate among 12 temperate tree species. Ecology 98: 2224-2235.
618 McCormack ML, Dickie IA, Eissenstat DM, Fahey TJ, Fernandez CW, Guo D, Helmisaari HS, Hobbie
619 EA, Iversen CM, Jackson RB, Leppalammi-Kujansuu J, Norby RJ, Phillips RP, Pregitzer KS,
620 Pritchard SG, Rewald B, Zadworny M (2015a) Redefining fine roots improves understanding of
621 below-ground contributions to terrestrial biosphere processes. New Phytol 207: 505-518. doi:
622 10.1111/nph.13363.
623 McCormack ML, Gaines KP, Pastore M, Eissenstat DM (2015b) Early season root production in relation
624 to leaf production among six diverse temperate tree species. Plant Soil 389: 121-129. doi:
625 10.1007/s11104-014-2347-7.
626 McCree KJ (1974) Equation for the rae of dark respiration of white clove and grain sorghum, as functions
627 of dry weight, photosynthetic rate, and tempearture. Crop Science 14: 509-514.
628 McMurtrie RE, Nasholm T (2018) Quantifying the contribution of mass flow to nitrogen acquisition by
629 an individual plant root. New Phytol 218: 119-130. doi: 10.1111/nph.14927.
630 Moyano FE, Atkin OK, Bahn M, Bruhn D, Burton AJ, Heinemeyer A, Kutsch WL, Wieser G (2009)
631 Respiration from roots and the mycorrhizosphere. In: WL Kutsch, M Bahn, A Heinemeyer (eds)
632 Soil Carbon Dynamics. Cambridge University Press, New York.
633 Oyewole OA, Inselsbacher E, Nasholm T (2014) Direct estimation of mass flow and diffusion of nitrogen
634 compounds in solution and soil. New Phytol 201: 1056-1064. doi: 10.1111/nph.12553.
635 Penning de Vries FWT (1974) Substrate utilization and respiration in relation to growth and
636 maintenance in higher plants. Netherlands Journal of Agricultural Science 22: 40-44.
637 Pinheiro J, Bates D, DebRoy S, Sarkar D, authors E, Heisterkamp S, Willigen BV, Ranke J, R-core (2022)
638 Package 'nlme'. In: V 3.1-155 (ed).
639 Poorter H (1994) Construction costs and payback time of biomass: A whole-plant perspective. In: J Roy,
640 E Garnier (eds) A Whole-Plant Perspective on Carbon-Nitrogen Interactions. SPB Academic
641 Publishing, The Hague.
642 Radville L, McCormack ML, Post E, Eissenstat DM (2016) Root phenology in a changing climate. J Exp
643 Bot 67: 3617-3628. doi: 10.1093/jxb/erw062.
644 Richter DD, Markewitz D, Trumbore SE, Wells CG (1999) Rapid accumulation and turnover of soil
645 carbon in a re-establishing forest. Nature 400: 56-58.
646 Sano T, Hirano T, Liang N, Hirata R, Fujinuma Y (2010) Carbon dioxide exchange of a larch forest after
647 a typhoon disturbance. Forest Ecology and Management 260: 2214-2223. doi:
648 10.1016/j.foreco.2010.09.026.
649 Scott-Denton LE, Rosenstiel TN, Monson RK (2006) Differential controls by climate and substrate over

650 the heterotrophic and rhizospheric components of soil respiration. Global Change Biology 12:
651 205-216. doi: 10.1111/j.1365-2486.2005.01064.x.
652 Subke J-A, Inglima I, Francesca Cotrufo M (2006) Trends and methodological impacts in soil CO2 efflux
653 partitioning: A metaanalytical review. Global Change Biology 12: 921-943. doi: 10.1111/j.1365-
654 2486.2006.01117.x.
655 Sun L, Hirano T, Yazaki T, Teramoto M, Liang N (2020) Fine root dynamics and partitioning of root
656 respiration into growth and maintenance components in cool temperate deciduous and
657 evergreen forests. Plant Soil 446: 471-486. doi: 10.1007/s11104-019-04343-z.
658 Sun LF, Teramoto M, Liang N, Yazaki T, Hirano T (2017) Comparison of litter-bag and chamber
659 methods for measuring CO2 emissions from leaf litter decomposition in a temperate forest.
660 Journal of Agricultural Meteorology 73: 59-67. doi: 10.2480/agrmet.D-16-00012.
661 Sweetlove LJ, Williams TC, Cheung CY, Ratcliffe RG (2013) Modelling metabolic CO(2) evolution--a
662 fresh perspective on respiration. Plant Cell Environ 36: 1631-1640. doi: 10.1111/pce.12105.
663 Tang X, Fan S, Zhang W, Gao S, Chen G, Shi L (2019) Global variability in belowground autotrophic
664 respiration in terrestrial ecosystems. Earth System Science Data 11: 1839-1852. doi:
665 10.5194/essd-11-1839-2019.
666 Thongo M'Bou A, Saint-André L, de Grandcourt A, Nouvellon Y, Jourdan C, Mialoundama F, Epron D
667 (2010) Growth and maintenance respiration of roots of clonal Eucalyptus cuttings: scaling to
668 stand-level. Plant Soil 332: 41-53. doi: 10.1007/s11104-009-0272-y.
669 Thornley JH (2011) Plant growth and respiration re-visited: maintenance respiration defined - it is an
670 emergent property of, not a separate process within, the system - and why the respiration :
671 photosynthesis ratio is conservative. Ann Bot 108: 1365-1380. doi: 10.1093/aob/mcr238.
672 Thornley JHM (1970) Respiration, growth and maintenance in plants. Nature 227: 304-305.
673 Warren JM, Hanson PJ, Iversen CM, Kumar J, Walker AP, Wullschleger SD (2015) Root structural and
674 functional dynamics in terrestrial biosphere models--evaluation and recommendations. New
675 Phytol 205: 59-78. doi: 10.1111/nph.13034.
676 Wieser G, Bahn M (2004) Seasonal and spatial variation of woody tissue respiration in a Pinus cembra
677 tree at the alpine timberline in the central Austrian Alps. Trees 18. doi: 10.1007/s00468-004-
678 0341-z.
679 Yazaki T, Hirano T, Sano T (2016) Biomass Accumulation and Net Primary Production during the Early
680 Stage of Secondary Succession after a Severe Forest Disturbance in Northern Japan. Forests 7.
681 doi: 10.3390/f7110287.
682 Yuan ZY, Chen HYH (2010) Fine Root Biomass, Production, Turnover Rates, and Nutrient Contents in
683 Boreal Forest Ecosystems in Relation to Species, Climate, Fertility, and Stand Age: Literature
684 Review and Meta-Analyses. Crit Rev Plant Sci 29: 204-221. doi:
685 10.1080/07352689.2010.483579.
686

687 **Statements and Declarations**

This study was supported by JPSP KAKENHI (17K20037) and the Environment Research and Technology Development Fund (JPMEERF20172005 and JPMEERF20202006) of Environmental Restoration and Conservation Agency of Japan. The authors have no relevant financial or non-financial interests to disclose. All authors contributed to the study conception and design. Material preparation, data collection and analysis were performed by Takashi Hirano, Rui Cui and Lifei Sun. The first draft of the manuscript was written by Takashi Hirano and all authors commented on previous versions of the manuscript. All authors read and approved the final manuscript. The datasets generated during the current study are available from the corresponding author on reasonable request.